Dopamine D1 Receptor Agonist and D2 Receptor Antagonist Effects of the Natural Product (−)–Stepholidine: Molecular Modeling and Dynamics Simulations

Wei Fu,*[†] Jianhua Shen,* Xiaomin Luo,* Weiliang Zhu,* Jiagao Cheng,* Kunqian Yu,* James M. Briggs,[‡] Guozhang Jin,* Kaixian Chen,* and Hualiang Jiang*[§]

*Drug Discovery and Design Centre, State Key Laboratory of Drug Research, Shanghai Institute of Materia Medica, Shanghai Institutes for Biological Sciences, Chinese Academy of Sciences, Shanghai 201203, People's Republic of China; [†]Department of Medicinal Chemistry, School of Pharmacy, Fudan University, Shanghai 200032, People' Republic of China; [‡]Department of Biology and Biochemistry, University of Houston, Houston, Texas, 77204-5001; and [§]School of Pharmacy, East China University of Science and Technology, Shanghai 200237, People's Republic of China

ABSTRACT   (−)–Stepholidine (SPD), an active ingredient of the Chinese herb *Stephania*, is the first compound found to have dual function as a dopamine receptor D1 agonist and D2 antagonist. Insights into dynamical behaviors of D1 and D2 receptors and their interaction modes with SPD are crucial in understanding the structural and functional characteristics of dopamine receptors. In this study a computational approach, integrating protein structure prediction, automated molecular docking, and molecular dynamics simulations were employed to investigate the dual action mechanism of SPD on the D1 and D2 receptors, with the eventual aim to develop new drugs for treating diseases affecting the central nervous system such as schizophrenia. The dynamics simulations revealed the surface features of the electrostatic potentials and the conformational "open-closed" process of the binding entrances of two dopamine receptors. Potential binding conformations of D1 and D2 receptors were obtained, and the D1-SPD and D2-SPD complexes were generated, which are in good agreement with most of experimental data. The D1-SPD structure shows that the K-167_EL-2-E-302_EL-3 (EL-2: extracellular loop 2; EL-3: extracellular loop 3) salt bridge plays an important role for both the conformational change of the extracellular domain and the binding of SPD. Based on our modeling and simulations, we proposed a mechanism of the dual action of SPD and a subsequent signal transduction model. Further mutagenesis and biophysical experiments are needed to test and improve our proposed dual action mechanism of SPD and signal transduction model.

INTRODUCTION

During the last decade, numerous efforts have been undertaken to discover drugs for treating psychomotor diseases, including the debilitating mental illness schizophrenia, which affects 0.5–1.5% of the worldwide population (1–4). It has been established that dopamine receptors (DRs) are primary targets for developing drugs to treat these diseases. DRs belong to the G-protein coupled receptor (GPCR) superfamily, transferring signals into cells through guanine nucleotide-binding regulatory G-proteins (4). The DRs can be classified into two major subfamilies, D1 and D2 receptors, according to their structural, pharmacological, and functional characteristics (4). Their functional domains have been defined, and the binding-site crevices have been identified by the substituted-cysteine-accessibility method (5–7). Although some studies revealed the structural features of D1 and D2 receptors that underlie their particular biophysical and pharmacological properties (6,8), many problems still remain unresolved due to experi-

mental limitations and the lack of three-dimensional (3D) structures.

Antagonists of the D2 receptor are believed to be potential drugs against the psychomotor diseases (9). Unfortunately, these antagonists (e.g., the neuroleptic haloperidol) have severe mechanism-related side effects, including induction of acute extrapyramidal symptoms (EPS), tardive dyskinesia, and problems of galactorrhea due to increase in prolactin release (10). In contrast, atypical antipsychotics with less EPS are effective in patients who are unresponsive to classical agents and may also have advantages in treating the more resistant negative symptoms of schizophrenia (10). The use of atypical antipsychotics was, however, found to have a high occurrence of a potentially fatal blood disorder called agranulocytosis (10). Therefore, discovering effective, safe antipsychotics remains a high priority (4,9,10).

The pathogenesis of schizophrenia was suggested to be related to dysfunction of the D1 receptor in the medial prefrontal cortex (mPFC), which is accompanied by D2 receptor hyperactivity in subcortical regions such as the ventral tegmental area (VTA) and the nucleus accumbens (NAc) (4). The D1 dysfunction was suggested to be responsible for the negative symptoms of schizophrenia, whereas the hyperactivity of the D2 receptor might lead to the positive symptoms of this disorder (4,5,11). Based on this hypothesis, antipsychotic

drugs with dual effect as a D1 receptor agonist and a D2 receptor antagonist would provide a new treatment for psychotic diseases (4).

An active compound, namely (−)–stepholidine (SPD), isolated from the Chinese herb *Stephania*, is to date the only drug with a dual effect as a D1 receptor agonist and a D2 receptor antagonist (4). SPD has high affinity for D1- and D2-like receptors but low affinity for 5-HT$_2$ receptors and α_2-adrenoceptors (4). The dual action of SPD has been demonstrated in both cortical and subcortical structures, including the mPFC, NAc, VTA, and basal ganglia dopamine systems (4). Moreover, clinic studies showed that SPD is superior to perphenazine in antipsychotic efficacy. Unlike perphenazine, SPD does not induce any EPSs (4), making SPD an attractive compound in studying the dual action mechanism of a chemical for developing novel antipsychotic drugs. However, the molecular basis of the dual action of SPD is obscure to date. Thus, exploring the dual action mechanism of SPD against D1 and D2 receptors at the atomic level is the first step toward developing more superior antipsychotic agents. Obviously, the 3D structures of D1 and D2 receptors are essential to figuring out the dual action mechanism. Unfortunately, these 3D structures are not currently available.

It has been widely recognized that molecular modeling and simulation are an excellent complement to experiments in explaining experimental results and providing clues for further experiments. Furthermore, it may reveal information that is not accessible by experiments (12). Recently, great success has been achieved in the field of structure prediction of GPCRs (13–15). For instance, some algorithms are capable of predicting the transmembrane (TM) structures (15–20). However, constructing appropriate conformational states of the extracellular or intracellular domains of GPCRs is still a tough job. Molecular dynamics (MD) simulations (21), taking advantage of iteratively tracking the trajectory of conformational change, could be used to simulate the binding process, to explore the binding conformation, and to map the binding mechanism at molecular and atomic levels. To the best of our knowledge, no long timescale MD simulation has been carried out so far on DRs. All this motivates us to carry out a computational study on D1 and D2 receptors to explore the mechanism of the dual action of SPD on these two receptors. Thus, homology modeling, automated molecular docking, and MD simulations have been integrated in this study. A homology modeling approach was used to construct 3D structures of D1 and D2 receptors. Automated docking was used to find possible binding sites for SPD against the receptors. The MD simulations, performed in a fully hydrated lipid bilayer environment, were carried out to address the following questions: How does SPD bind to the D1 and D2 receptors? How does SPD regulate the signal transduction of the D1 receptor? What is the fundamental basis underlying the dual action of SPD?

MODELING AND SIMULATION METHODS

Strategy of modeling and simulation

Experiments demonstrated that the sequences of aminergic receptors, viz. dopamine, α-adrenergic, β-adrenergic, and serotonin receptors, are highly conservative within the TM domains, which dictate the common ligand-binding sites of these receptors (22). However, experimental data also suggest that different binding interactions of ligands to one receptor lead to different receptor conformations (10). The small changes in ligand structure may affect its interactions with the receptor and, hence, the receptor activation (10). Thus, we faced two difficulties: 1), how to construct 3D models of the D1 and D2 receptors, and 2), how to identify the binding conformations of the two receptors with SPD. To solve these problems, we integrated several modeling and simulation methods in this study. The computational pipeline is outlined in Fig. S1 in the Supplementary Material. Briefly, the computational flow is as follows:

1. The 3D models of the D1 and D2 receptors were constructed using a homology-modeling approach based on the x-ray crystal structure of bovine rhodopsin.
2. Two 10-ns MD simulations were carried out respectively on the constructed D1 and D2 receptor models, embedded in a hydrated POPC (palmitoyloleoylphosphatidylcholine) bilayer.
3. To find the probable SPD binding conformations of D1 and D2 receptors, SPD was docked into numerous minimum-energy conformations isolated from the MD trajectories of the two receptors by using the molecular docking approach, including prediction of the binding free energy between SPD and each selected conformation of the receptors. Conformations of the two receptors with lowest binding free energies to SPD were selected as the initial structures for further simulations.
4. Two additional 10-ns MD simulations were conducted on the initial structures of SPD-D1 and SPD-D2 complexes, resulting from the above docking calculations, embedded in a hydrated POPC bilayer.
5. The ligand-receptor interaction and the dual action mechanism of SPD were explored by analyzing all of the modeling and simulation results.

Homology modeling for the 3D models of D1 and D2 receptors

Bovine rhodopsin, a member of the GPCR superfamily, was structurally determined at a resolution of 2.80 Å (Protein Data Bank entry 1F88) (17). This x-ray structure of GPCRs provides a solid template for modeling the 3D structures of other GPCRs (7). To obtain a reliable sequence alignment, 64 sequences of dopamine-type receptors downloaded from http://www.gpcr.org/7tm were used. Residues were numbered according to the generalized numbering scheme proposed by Ballesteros and Weinstein (22). To facilitate the comparison among the aligned residues in various GPCRs, the most conserved residue in transmembrane X is given the index number X.50, and residues within a given TM are then indexed relative to the "50" position.

The MODELLER program encoded in InsightII (23) was employed to assemble the 3D models of the α-helix bundles of D1 and D2 receptors by using the x-ray crystal structure of bovine rhodopsin as a template. The FASTA program (24) was used to identify sequence homology through an in-house database (15) containing 700 loops and proteins with medium to high sequence identity. ClustalW (25) was then used to determine the fragments that have higher homology with the loops of D1 and D2 receptors. A reasonable fragment conformation was chosen from the top 10 candidates that have the lowest root mean-square (RMS) values and considerable geometrical compatibility. The conserved disulfide bond between residues Cys-3.25 at the beginning of TM III and Cys_EL-2 in the middle of extracellular loop 2 (EL-2) was also created. Energy minimizations of the models were carried out using the Discover module encoded in InsightII with the same parameters as that of our previous studies (12).

Molecular dynamics simulations

The MD simulations were performed using the GROMACS package version 3.1.4 with the GROMOS96 force field. (26,27) (www.gromacs.org). The molecular topology file for SPD was generated with PRODRG (28) (http://davapc1.bioch.dundee.ac.uk/programs/prodrg/prodrg.html). The partial atomic charges of SPD were determined by using the CHelpG method (29) implemented in the Gaussian98 program (30) with the DFT/B3LYP/6-311G** basis set. For MD simulations, the four models (unliganded D1, unliganded D2, SPD-D1, and SPD-D2 complexes) were embedded in a hydrated POPC lipid bilayer. The procedure and parameters for constructing the receptor/hydrated POPC systems are similar to those used in previous membrane protein simulations (31–33). Fig. 1 shows, taking the SPD-D1 complex as an example, the structural model of the receptor/POPC/water systems. Before MD simulations, energy minimizations were performed on the four receptor/hydrated POPC systems first for all water molecules to remove their poor contacts with protein atoms, then for the whole system until the maximum force was <10.00 kcal/mol-Å.

The solvent (water and POPC) molecules of each initial system were equilibrated with protein structures by constraining the solute (D1 or D2) at 300 K for 20 ps. Then the protein was equilibrated for 5 ps and the solvent molecules were constrained at 10, 50, 100, 200, and 298 K. Afterward, each system was equilibrated for 250 ps without any constraints. To maintain the systems at a constant temperature of 300 K, the Berendsen thermostat (34) was applied using a coupling time of 0.1 ps for the bulk water and POPC. The pressure was maintained by coupling to a reference pressure of 1 bar. The values of the anisotropic isothermal compressibility were set to 4.5×10^{-5}, 4.5×10^{-5}, 4.5×10^{-5}, 0, 0, 0 bar^{-1} for xx, yy, zz, xy/yx, xz/zx, and yz/zy components, respectively, for water and POPC simulations. The lengths of all bonds, including those to hydrogen atoms, were constrained by the LINCS algorithm (26). Electrostatic interactions between charged groups within 9 Å were calculated explicitly, and long-range electrostatic interactions were calculated using the particle mesh Ewald method (35) with a grid width of 1.2 Å and a fourth-order spline interpolation. A cutoff distance of 14 Å was applied for the Lennard-Jones interactions. Numerical integration of the equations of motion used a time step of 2 fs with atomic coordinates saved every 1 ps for later analysis. To neutralize the modeled systems, 13, 9, 12, and 8 Cl^{-} ions were added to the molecular systems of the free D1, D2, SPD-D1, and SPD-D2 complexes, respectively. Finally, four 10-ns MD simulations were performed on these systems under the periodic boundary conditions in the NPT canonical ensemble.

Molecular docking and binding energy calculation

The geometry of the SPD ligand was built based on its crystal structure (36) and optimized at the DFT/B3LYP/6-311G** level. This protonated structure features the R configuration and a half-chair conformation of rings B and C. The dihedral angle between rings A and D is 158°. The molecular docking program AutoDock3.05 (37) was employed to probe the possible SPD-

binding sites of the energy-minimum conformations of the D1 and D2 receptors derived from the MD trajectories.

RESULTS

3D structures of D1 and D2 receptors

Sequence alignment (Fig. S2 in the Supplementary Material) indicates that the sequence identity and similarity are 21.8% and 47.8%, respectively, for the TMs between rhodopsin and the D1 receptor, 26.1% and 54.4% for the TMs between rhodopsin and D2 receptor, and 44.5% and 66.4% between the D1 and D2 receptors themselves. Based on the high homology revealed by sequence alignments, the 3D models of the D1 and D2 receptors were assembled taking the x-ray crystal structure of bovine rhodopsin as a template. The PROCHECK (38) statistics showed that 90% of the residues in both the D1 and D2 models were in either the most favored or in the additionally allowed regions of the Ramachandran map (Fig. S3 in the Supplementary Material), suggesting that the overall main chain and side chain structures are all reasonable. The WHATIF (39) validation shows acceptable RMS Z-scores. All of these data suggest that the models obtained through our homology modeling are reasonable. Two kinds of interaction networks are observed in D1 and D2, i.e., aromatic residue clusters (Fig. S4) and hydrogen bond (H-bond) network (Table S1). The presence of hydrophobic cluster and H-bond interaction with TM III and TM VII in D1 could allow relative movement of TM VI. The specific H-bonds cluster at the bottom of TM III and TM V is observed consisting of R-3.50 and E-6.30. It is conserved in both D1 and D2 receptors, and the DRY motif of TM III may be relevant to the activation or inactivation of the receptor.

The extracellular loop 1 (EL-1) and extracellular loop 3 (EL-3) are typically short in all aminergic GPCRs. In contrast, EL-2 is significantly longer and may reach into the active site crevice and form a lid over the bound ligand. There is a highly conserved disulfide bond between the conserved Cys_e2 at the middle of EL-2 and Cys-3.25 at the beginning of TM III. Thus in D1 and D2 receptors, the stretches of only 4–5 residues between Cys_e2 and extracellular end of TM5 are in an extended state to reach two sides. It is noteworthy
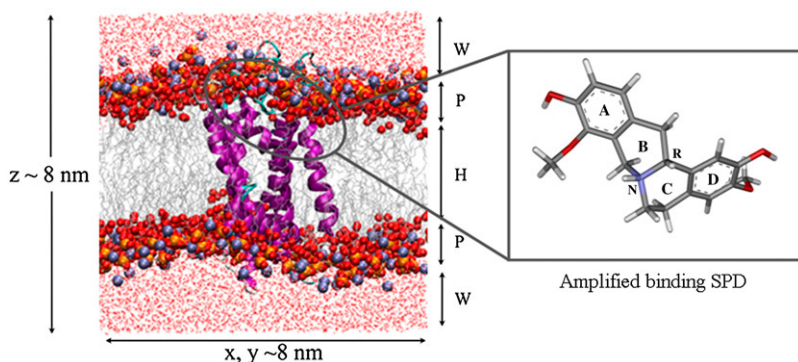

FIGURE 1 Overview of the SPD-D1/POPC/water system. D1 is shown in ribbon; the hydrophobic chains of bilayer lipids are labeled H; and the lipid carbonyl oxygen atoms, choline N atoms, and P atoms are represented in a space fill model (labeled *P*), and water as W; the 3-D size of the whole system was also labeled. The SPD in binding site was amplified and shown in a stick model.

that there are 13 residues in the EL-2 loop of the D2 receptor, whereas 26 residues exist in the EL-2 loop of the D1 receptor. The main difference in EL-2 mainly comes from the upstream preceding conserved Cys_e2 (Fig. S2), which is far away from the active site crevice. In addition, there are six residues longer in the EL-3 of the D1 receptor than that of the D2 receptor. Though the lengths of EL-2 and EL-3 are different, they are flexible and function as the conformational switch to catch the outcoming ligands (see the discussion in the next paragraph).

Open-closed conformational changes of free D1 and D2

The MD simulations of the free D1 and D2 systems showed that, for all of the systems, the temperature, mass density, and volume are relatively stable after 2 ns. About then, the fluctuation scale became much smaller for both the RMS deviations of the C_α atoms and potential energies (Fig. 2) of the two simulation systems, indicating that the molecular systems were well behaved thereafter.

When analyzing the MD trajectories, a striking ''open-closed'' conformational change is observed from the extracellular side for both the D1 and D2 receptors, as demonstrated in Fig. 3. Further examination reveals that such an ''open-closed'' event can be attributed mainly to large conformational changes in the EL-2 and EL-3, coupled with the connecting TM helices. Typically, EL-2 and EL-3 act as ''lips'' of mouth-like entrances of the binding sites of these two receptors. This can be demonstrated by the fluctuations of critical distance between K-167 at EL-2 and E-302 at EL-3 (K-167-E-302 pairing), which is an objective monitor of the width of the entrance. The open and closed conformations are shown in the dotted lines in Fig. 2. Taking D1 as an example, the opening event at ~2630 ps for the ''mouth'' corresponds to changes in the K-167-E-302 pairing distance (Fig. 4 A), which reaches one of the ''peak'' points as shown in Fig. 6. As time proceeds, the ''mouth'' becomes gradually closed at ~4210 ps and the distance between K-167-E-302 decreases to a local minimum. Such synchronization between the ''open-closed'' conformational changes of the

whole D1 receptor and peak-minimum distance changes of K-167-E-302 (Fig. 4 A) occurred three times during our 10-ns MD simulations. Quite similar open-closed conformational changes were also seen for the free D2 (Fig. 3 B). These dynamic properties suggest that there are at least two distinct conformations for both D1 or D2, and the spontaneous oscillation between these two conformational states appears to be an intrinsic phenomenon. Our observation is in agreement with experimental mutagenesis studies in which it was postulated that GPCRs exist in an equilibrium between two interchangeable conformational states (40,41). One of the obvious advantages of this type of dynamical behavior of the binding site entrances (open-closed) is that it enables the receptors to easily capture different ligands (agonists and antagonists) or different conformations of a ligand, as will be discussed later.

Tracing the MD trajectory of both the D1 and D2 receptors revealed a portion of the atomic-level mechanism of the open-closed motion. A hydrogen-bond (H-bond) network exists between the charged side chains of K-167 and E-302. At the beginning of MD simulation, the positively charged side chain of K-167 forms direct H-bonds and two indirect (water-bridged) H-bonds with the negatively charged side chain of E-302 (Fig. 5 A). As the simulation proceeds, the side chain of the E-302 turns away from K-167, breaking the H-bond network. At ~2630 ps, all of the H-bonds between K-167 and E-302 are gone. Meanwhile, K-167 gradually approaches D-173 of EL-2, forming a new H-bond network via water bridges (Fig. 5 B) which lasts ~1 ns. K-167-E-302 switches back to the pairing state similar to that in Fig. 5 A, and the H-bond network is restored. K-167 changes partners frequently, either E-302 or D-173, staying with D-173 when the ''mouth'' is open and with E-302 when the ''mouth'' is closed. Therefore, the H-bond network between K-167 and E-302 seems to act as a ''bolt''—its position controls whether the ''mouth'' is open or closed.

Binding conformations of SPD in the D1 and D2 receptors

To identify the most probable binding conformations of SPD to the D1 and D2 receptors, 10 potential binding conformation
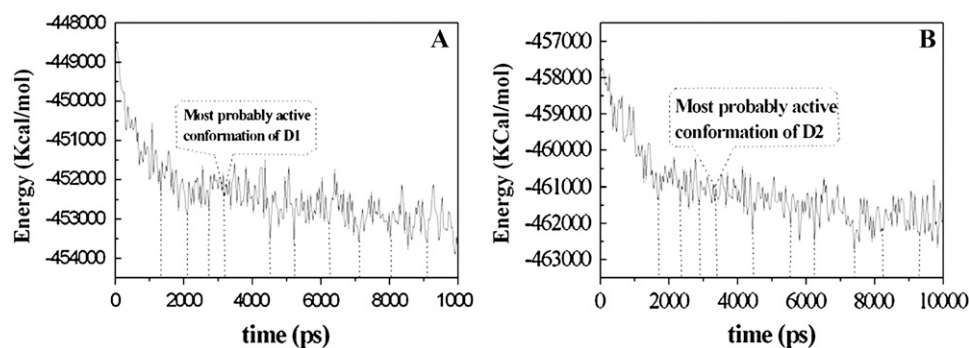

FIGURE 2 Energy changes along MD simulations. (A) D1 simulation system. (B) D2 simulation system. Ten conformations shown in dotted line were identified with two criteria: lower potential energy and obvious geometrical difference among different conformations. Among them, the conformations at 2630 ps in the MD trajectory of the unliganded D1 and that at 3310 ps in the MD trajectory of unliganded D2 have the lowest binding energies toward SPD and were selected as the conformations most probably active.
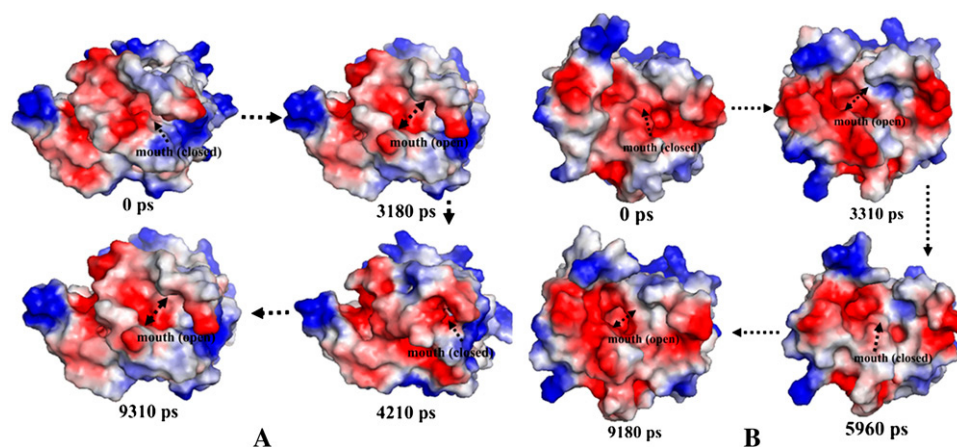
FIGURE 3 Representative conformations of the D1 (*A*) and D2 (*B*) receptors during the open-closed process of the binding site as observed from MD simulations. A dashed arrow line indicates the position of the ''mouth'', and a double arrow dashed line shows the ''mouth'' opening. All of the conformations are shown in the style of molecular surface colored by electrostatic potential. The red color stands for negative electrostatic potential, and the blue for positive potential.

candidates of DRs were identified from each of the MD trajectories of the unliganded D1 and D2 receptors (*dotted lines* in Fig. 2) with two criteria: lower potential energy and obvious geometrical difference among different conformations. Then SPD was docked into the binding cavities of these 10 conformations of each receptor and the binding energies were estimated by means of AutoDock3.05 (37). Both the binding mode and binding affinity between SPD and DRs were used to guide the selection of the conformation that is most likely to be active. From among 10 candidates, the conformations were selected as the possible conformation candidates if their main binding modes are in agreement with known mutagenesis experiments. From these possible conformation candidates, the conformation having the lowest binding energy toward SPD was selected as the conformations most likely to be active for each DR. The predicted lowest binding free energy of SPD for D1 is -12.8 kcal/mol and -11.7 kcal/mol, respectively. Although there are deviations between the experimental value (-10.8 kcal/mol and -9.6 kcal/mol) (42–45) and predicted data, the general trend observed in predicated binding free energies is that SPD binds to D1 more strongly than to D2. The errors in predicting binding affinities mainly come from the homology models of DRs and the imperfect empirical parameters in AutoDock 3.05 for estimating binding affinity.

Dual action mechanism of SPD with dopamine D1 and D2 receptors

The structural determinant of pharmacological specificity of SPD

The dynamics of the interactions between SPD and D1 or D2 was investigated to understand the agonistic and antagonistic mechanism of SPD.

The distances between the key residues in the active sites were monitored and used to delineate the dynamical change of the active site among the bound complexes. Most distances fluctuate a little bit in complexes SPD-D1. It shows that SPD packs well with the side chains of residues in the binding cavity of D1. In the SPD-D2 complex, there is an interesting conformational change around the ligand. The side chains of F-6.52 and H-6.55 come near the aromatic rings A and D of SPD, apparently induced by hydrophobic interactions among these groups and the bending of rings A and D toward side chains of F-6.52 and H-6.55. There is also an electrostatic attraction between the protonated side chain of H-6.55 and the electron-rich group of ring A and atom O2 of SPD (Fig. 6 *D*). The conformational bending of SPD and the aromatic packing with the side chains of F-6.52 and H-6.55 appear to hold SPD against helix VI, constraining it after SPD binding. In comparison, there is no such
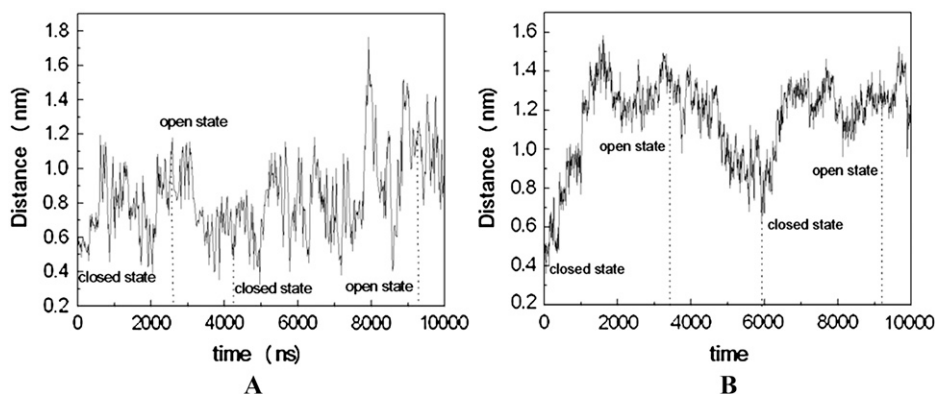

FIGURE 4 Distance fluctuations during the MD simulations. (*A*) Distance from N_ζ of K-167 (EL-2) to C_δ of E-302 (EL-3) of the D1 receptor; (*B*) distance from C_γ of D-178 (EL-2) to the centroid of the aromatic side chain of Y-408 (EL-3) of the D2 receptor. The open and closed conformations in Fig. 3 are shown in the dotted lines in Fig. 2.
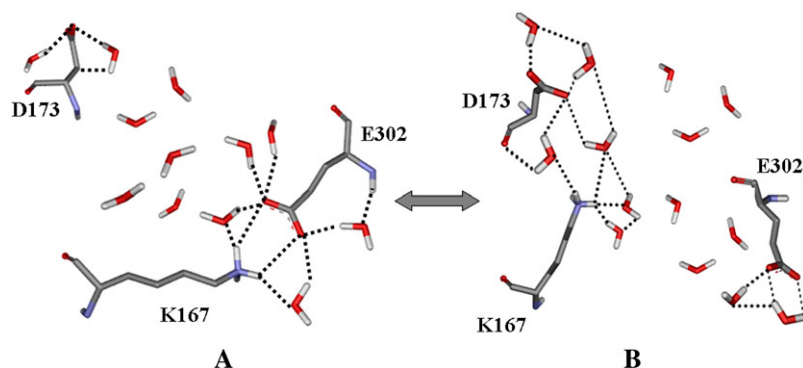
FIGURE 5 Hydrogen-bonding network among K-167, D-173, E-302, and bridging water molecules in D1.

conformational packing in the dynamic SPD-D1 complex, so we consider this packing effect in the dynamic SPD-D2 complex to be a structural determinant in the antagonism of SPD with the D2 receptor, which will be described in detail later.

The agonistic and antagonistic conformations of SPD

There is only a small difference between the initial conformations of SPD in the complexes with D1 and D2. By mutual conformational adjustment during the first ~5 ns of dynamics, the conformation of SPD in the D2 binding cavity becomes quite different from that in the D1 binding cavity (Fig. 6, *C* and *D*). The first adjustment was to the dihedral angle between rings A and D. In the SPD-D2 complex, ring A of SPD becomes almost perpendicular to ring D (dihedral angle of 98°), whereas the relative position of these two rings in SPD still maintains planarity (dihedral angle of 150°) in the SPD-D1 complex. The second adjustment is reflected in the different interactions between SPD with D1 and D2. As

shown in Fig. 6, the interactions between ring A of SPD and the surrounding residues of D1 are mainly aromatic stacking with the side chains of W-3.28, W-7.40, and W-7.43, plus direct hydrogen bonding between the hydroxyl group on ring A of SPD with Nξ1 of W-3.28 (Fig. 6, *C* and *E*). In the SPD-D2 complex, ring A of SPD has much stronger electrostatic and hydrogen-bonding interactions with the protonated H-6.55. The role of H-6.55 in stabilizing the bent SPD conformation in the D2 binding cavity becomes more important because the N-6.55 at the same position in the D1 receptor is not involved in any interactions with SPD.

Energies of the agonistic and antagonistic conformations of SPD

We next investigated the energetics of the different bioactive conformations of SPD in the different receptors, D1 and D2. Quantum mechanical methods were employed to calculate
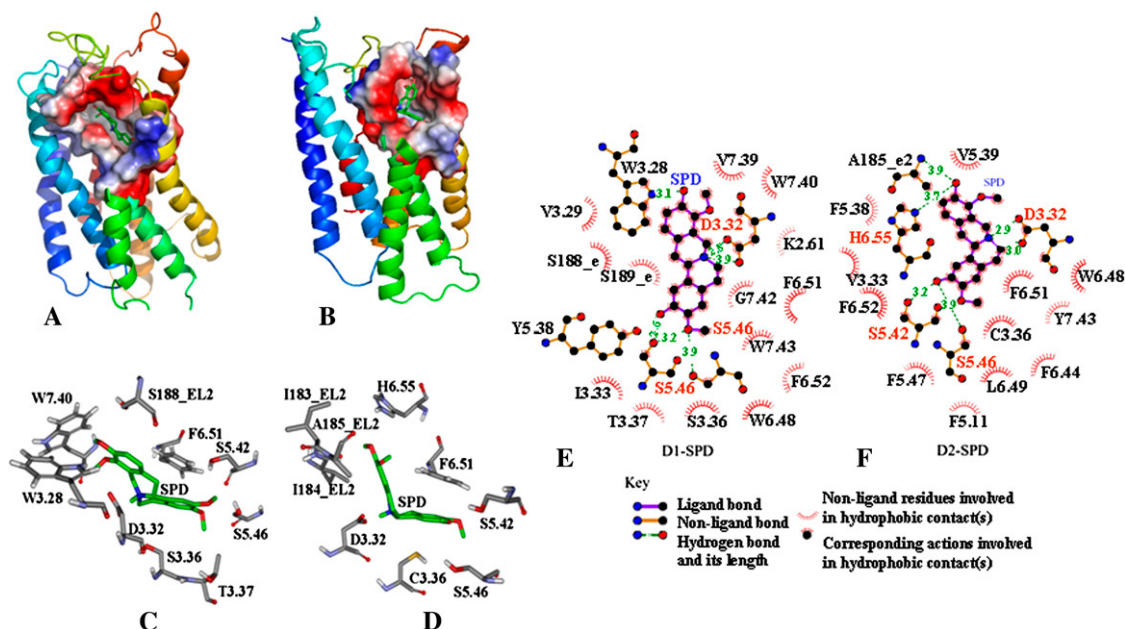

FIGURE 6 Binding modes of SPD in the D1 (*A*, *C*, and *E*) and D2 (*B*, *D*, and *F*) receptors. (*A* and *B*) The models of D1-SPD and D2-SPD. The active sites were displayed as an electrostatic surface. (*C* and *D*) The important residues in the active sites of two complexes and SPD were rendered in stick representation. (*E* and *F*) Schematic depiction of the main interactions between SPD with D1 and D2.

molecular energies at the DFT/B3LYP/6-311G** level using the Gaussian 98 program. The transition state conformation of SPD between the agonistic and antagonistic conformations was located by the synchronous transit-guided quasi-Newton methods (46) at the same level. Fig. 7 shows that there is only a small energy barrier, 1.55 kcal/mol, between the conformation of SPD in the D1 complex and the transition state conformation. The energy barrier between the conformation of SPD in the D2 complex and the transition state conformation is 1.02 kcal/mol. These small energy differences demonstrate that the transition of SPD from the agonist conformation to antagonist one is relatively facile. In other words, SPD intrinsically has the capacity for dual functional when associating with different DRs (D1 and D2).

Dynamical helix movement of the D1 receptor upon SPD binding

In corresponding to the agonizing and antagonizing effects of SPD, the TM helices of D1 and D2 take different extents of motion. Taking the radius of gyration (Rg) as an example (Fig. 8), the Rg of helices 1–7 in the SPD-D1 complex gradually increases after ~3.0 ns and maintains a value of 1.775 nm from there until the end of the MD simulations. In comparison, the Rg value of the SPD-D2 complex changes slightly and maintains almost the same value as for the free D2 receptor. Usually, the larger the Rg, the greater the extent of the range of motion of the structure. The essential dynamics analyses (47) performed on the complete MD trajectories of the complexes helped us locate the most drastic motions among helices. Two projected structures representing the minimal and maximal amplitudes along the first eigenvector were selected and superimposed with each other (Fig. 9). The relative motion among helices is different before and after SPD binding in two receptors. In comparison with the SPD-D2 complex, the binding of SPD to the D1 receptor (Fig. 9, *A* versus *C*) results in the outward movement of seven TM

FIGURE 7 Energy barrier between the agonistic and antagonistic conformers of SPD calculated with B3LYP/6311g**. The calculated energy is 1.55 kcal/mol after the zero-point vibrational energy (ZPVE) correction.

helices, especially TM6 and TM7, SPD-D1 complex is quite relaxed. Among seven TM helices in the SPD-D1 complex, TM6 and TM7 have the largest outward movement toward the surrounding lipids (Fig. 9 *A*). On the other hand, the SPD-D2 complex is quite conservative (Fig. 9, *B* and *D*) in the motion of its helices. The dramatic movement of the TM6-TM7 helices in the SPD-D1 complex appears to result from the agonistic effect of SPD and distally propagates into the intracellular end.

DISCUSSION

In this article we integrated homology modeling, MD simulation, automated docking, and density function theory to understand the agonistic and antagonistic mechanism of SPD and the activation process of the D1 receptor. So far, only the structure of the bovine rhodopsin receptor was characterized in the GPCR family. The identities between rhodopsin and DRs D1 and D2 are ~25%. Though we carefully built D1 and D2 models and checked them by several programs of structural validation and all available experimental data, the models are still fuzzy. Furthermore, the timescale of our MD simulations is short compared to the real biological process of DRs. However, the current models are supported by most known mutagenesis experiments, and our MD simulations give the trend of the motion of the proteins. Since it is very difficult to characterize the structure of membrane protein and its dynamical characteristic experimentally, it is a useful complement for investigation of structural and functional characteristic of the GPCR family and provides clues in understanding the signal transduction process of DRs. In particular, the obtained agonistic and antagonistic mechanism of SPD can provide practical guidance for the design of dual function lead compounds for D1/D2 receptors.

Interpretation of mutation data

Without high resolution structural information for the D1 and D2 receptors, site-directed mutagenesis is usually employed to explore the molecular mechanism of receptor activation and signal transduction by ligand binding. To date, several residues in either the D1 or D2 receptors have been revealed to be critical for ligand binding. For example, D-3.32 (D-3.32G, D-3.32N, and D-3.32C) has been shown to be critical to SPD binding for both the D1 and D2 receptors via mutagenesis studies (5,6). Consistent with experimental data, our models for both SPD complexes with the D1 and D2 receptors demonstrate that D-3.32 acts as a hydrogen-bond acceptor and forms electrostatic interactions with the protonated SPD. Our complex models also show that the side-chain hydroxyl group of either S-5.42 or S-5.46 forms a hydrogen-bond with the hydroxyl group on ring D of SPD in both the D1 and D2 complexes. Removing the hydroxyl group of S-5.42 or S-5.46 will undoubtedly reduce the binding affinity of SPD with these two DRs. Cox et al. (40)
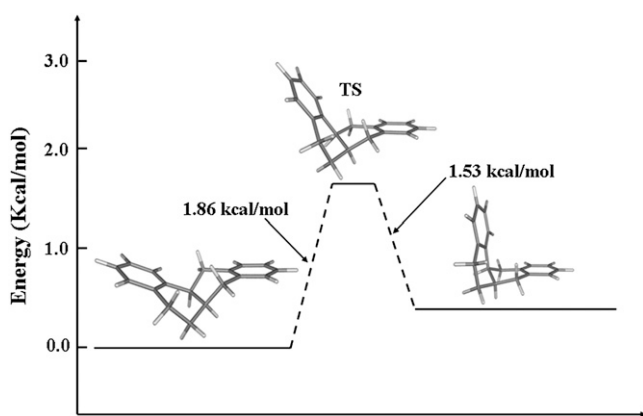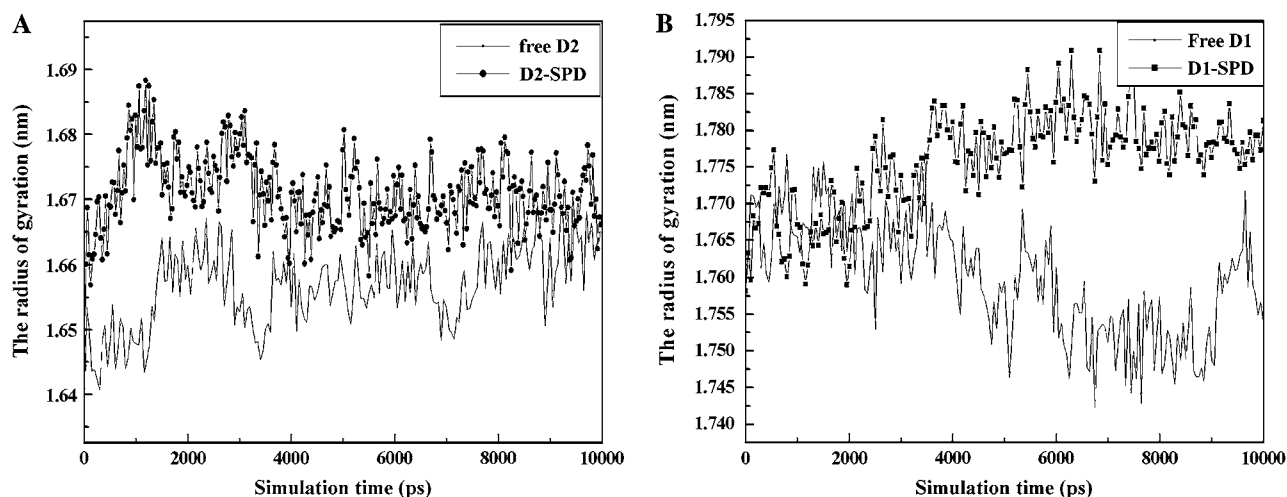
FIGURE 8 Time-dependent Rg of the four models. (*A*) D1 and D1-SPD. (*B*) D2 and D2-SPD.

and Tomic et al. (2) reached the same result on these two residues via S-5.42A and S-5.46A mutations and related functional studies. The importance of W-7.40 and W-7.43 in the D1 receptor can be attributed to their involvement in aromatic packing with rings A and B of SPD (Fig. 6). This is why the W-7.40A and W-7.43A mutations performed by Roth et al. (48) resulted in a decrease in binding affinity of the D1 receptor with its agonists. Our SPD-D2 complex model and its dynamic properties have illustrated why the D2 receptor is antagonized by SPD, that is, because electrostatic interactions with the protonated H-6.55 and the

aromatic stacking with F-6.52 made it difficult for helix VI and its neighbors to move. Such a move of interaction is in accord with the findings of Woodward et al. and others (49–51): H-6.55C and H-6.55L mutations caused a remarkable decrease in antagonist binding of the D2 receptor. Combined with these experimental results, it can be inferred that residues such as D-3.32, S-5.42, S-5.46, S-3.36, H-6.55, W-7.40, and W-7.43 should be structural determinants for the pharmacological specificity of the dual actions of SPD against the D1/D2 receptors.

Proposed signal transduction model of the D1 receptor

Based on our structural modeling and MD simulations, a stepwise signal transduction model of D1 was proposed (Fig. 10). Since the model of D1 was built based on the bovine rhodopsin, which has low identity with DRs (~25%), and the MD simulation is short compared with the real biological process of D1 motion, we should say that this model is somewhat uncertain. However, our model and simulations were supported by most known mutagenesis experiments. It provides some useful information/clues for researchers who investigate the activation process of the GPCR family. Further biophysical experiments are needed to test and improve this model.

Typically, the D1 receptor adopts the inactive state R through its intramolecular interaction and transits between several energy minima conformations by molecular thermodynamic motion. As the protonated SPD diffuses to the extracellular mouth of the binding cavity of the D1 receptor, a kind of electrostatic signal is transmitted to the molecular surface of D1 and promotes the disruption of the K-167-E-302 salt bridge. The electrostatic attraction between the negatively charged region of the D1 receptor and positively charged SPD assists in their initial association (Rt_1 state).
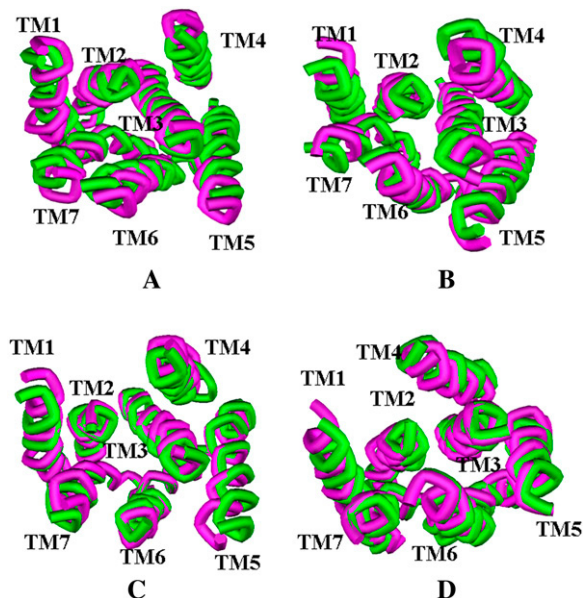

FIGURE 9 Largest anharmonic motions of the TM helices (viewed intracellularly) identified by essential dynamics analysis. (*A*) D1-SPD. (*B*) D2-SPD. For comparison, the minimum motion of helices is shown in green, and the maximum is colored in purple for both complexes.
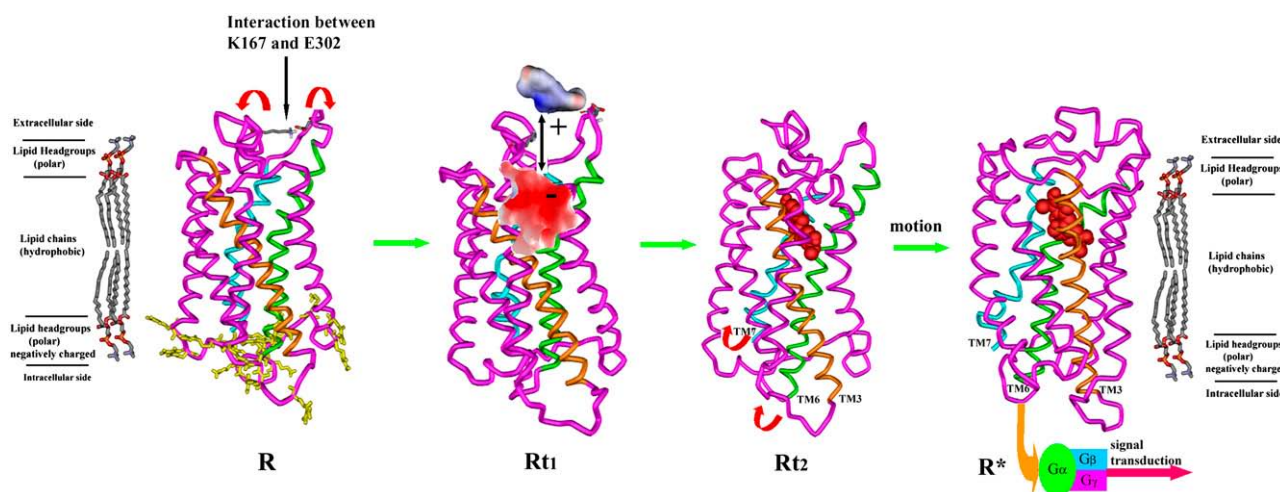
FIGURE 10 Signal transduction model of the D1 receptor by an SPD-like agonist. R represents the dynamic state, Rt_1 and Rt_2 are transitional states before receptor activation, and R* refers to the activated state ready to couple with intracellular G-proteins.

Further nestling of SPD into the binding cavity brings about a dramatic outward movement toward lipid in TM6 and TM7 (Rt_2 state). Through this induced conformational shift, the receptor is activated and couples with the α-subunit of the intracellular G-protein (R* state), transferring extracellular signals to the intracellular G-protein. This stepwise signal transduction model was supported by the currently accepted postulate about the activation of GPCRs; that is, GPCRs exist in an equilibrium between two interchangeable conformational states, namely a dynamic R state and an activated R* state (40,41), and there should be considerable conformational movement in TM6 and TM7 after agonist binding (17,19,52–54).

Significance to future drug discovery targeting the D1/D2 receptors

DRs remain attractive and challenging drug targets when searching for potential therapeutics of psychological diseases (4,41). Our demonstration of a potential molecular mechanism for the dual function of SPD as an agonist of D1 and an antagonist of D2 provides practical guidance in the design of novel lead compounds. We already have made some promising progress along these lines via our screening for novel SPD-like compounds combined with experimental testing (W. Fu, W. Zhu, and H. Jiang, unpublished data). Our computational results suggest that any small compound able to pack well with W-7.40 and W-7.43 in the D1 receptor and pack with H-6.55 in D2 may exhibit dual activity against the D1 and D2 receptors, as does SPD.

CONCLUSIONS

We report herein four 10-ns MD simulations of the unliganded D1 and D2 receptors and D1-SPD and D2-SPD complexes, all simulated in a lipid bilayer membrane. Distribution of the electrostatic potentials on the molecular surface and the conformational ''open-closed'' transition of the D1 and D2 receptors were addressed by the MD simulations. The K-167_EL-2-E-302_EL-3 salt bridge in the D1 receptor plays an important role in the conformational change of extracellular domain and in the binding of SPD. The binding of SPD to the D1 receptor causes a structural relaxation, which is an early step in the activation of GPCRs. Major and significant structural differences were seen in the TM6 and TM7 domains in the D1-SPD complex. In particular, TM6 exhibits the most significant motion during D1 receptor activation.

A detailed molecular level mechanism of the D1 agonist and D2 antagonistic action of SPD has been delineated. Our models indicate that the agonistic binding site in D1 and the antagonistic binding site in D2 share a common binding region in the structurally aligned receptors. However, SPD takes on two different bioactive conformations, one in the agonistic complex with D1 and the other in the antagonistic complexes with D2. The structural determinants for the pharmacological specificity of dual action of SPD were uncovered from the modeling and simulations. Combined with all the available experimental data, it can be concluded that residues H-6.55, W-7.40, and W-7.43 must be structural determinants for differentiating the pharmacological dual specificities of SPD for the D1 and D2 receptors. Finally, a potential signal transduction mechanism of the D1 receptor was proposed. Further mutagenesis and biophysical experiments are needed to test and improve our dual action mechanism of SPD and stepwise signal transduction model.

Our results have already been used in database searching to identify new candidate compounds with dual actions based on our identified D1 agonist and D2 antagonist conformations. Several molecular leads for the eventual treatment

of diseases affecting the central nervous system, such as schizophrenia, have been selected and are undergoing further experimental testing (W. Fu, W. Zhu, and H. Jiang, unpublished data).

SUPPLEMENTARY MATERIAL

To view all of the supplemental files associated with this article, visit www.biophysj.org.

REFERENCES

1. Pollock, N. J., A. M. Manelli, C. W. Hutchins, M. E. Steffey, R. G. Mackenzie, and D. E. Frai. 1992. Serine mutations in transmembrane V of the dopamine D1 receptor affect ligand interactions and receptor activation. *J. Biol. Chem.* 267:17780–17786.

2. Tomic, M., P. Seeman, S. R. George, and B. F. O'Dowd. 1993. Dopamine D1 receptor mutagenesis: role of amino acids in agonist and antagonist binding. *Biochem. Biophys. Res. Commun.* 191:1020–1027.

3. Payne, S. L., A. M. Johansson, and P. G. Strange. 2002. Mechanisms of ligand binding and efficacy at the human D2(short) dopamine receptor. *J. Neurochem.* 82:1106–1117.

4. Jin, G. Z., Z. T. Zhu, and Y. Fu. 2002. (−)–Stepholidine: a potential novel antipsychotic drug with dual D1 receptor agonist and D2 receptor antagonist actions. *Trends Pharmacol. Sci.* 23:4–7.

5. Mansour, A., F. Meng, J. H. Meador-Woodruff, L. P. Taylor, O. Civelli, and H. Akil. 1992. Site-directed mutagenesis of the human dopamine D2 receptor. *Eur. J. Pharmacol.* 227:205–214.

6. Javitch, J. A., D. Fu, J. Chen, and A. Karlin. 1995. Mapping the binding-site crevice of the dopamine D2 receptor by the substituted-cysteine accessibility method. *Neuron.* 14:825–831.

7. Ballesteros, J. A., L. Shi, and J. A. Javitch. 2001. Structural mimicry in G protein-coupled receptors: implications of the high-resolution structure of rhodopsin for structure-function analysis of rhodopsin-like receptors. *Mol. Pharmacol.* 60:1–19.

8. Shi, L., and J. A. Javitch. 2002. The binding site of aminergic G protein-coupled receptors: the transmembrane segments and second extracellular loop. *Annu. Rev. Pharmacol. Toxicol.* 42:437–467.

9. Oerther, S., and S. Ahlenius. 2000. Atypical antipsychotics and dopamine D1 receptor agonism: an in vivo experimental study using core temperature measurements in the rat. *J. Pharmacol. Exp. Ther.* 292:731–736.

10. Kulagowski, J. J., H. B. Broughton, N. R. Curtis, I. M. Mawer, M. P. Ridgill, R. Baker, F. Emms, S. B. Freedman, S. Marwood, S. Patel, C. I. Ragan, and P. D. Leeson. 1996. 3-[(4-(4-Chlorophenyl)piperazin-1-yl)-methyl]-1 H-pyrrolo-2,3-b-pyridine: an antagonist with high affinity and selectivity for the human dopamine D4 receptor. *J. Med. Chem.* 39:1941–1942.

11. Pugsley, T. A., Y. H. Shih, S. Z. Whetzel, K. Zoski, D. V. Leeuwen, H. Akunne, R. Mackenzie, T. G. Heffner, D. Wustrow, and L. D. Wise. 2002. The discovery of PD 89211 and related compounds: selective dopamine D4 receptor antagonists. *Prog. Neuropsychopharmacol. Biol. Psychiatry.* 26:219–226.

12. Fu, W., M. Cui, J. M. Briggs, X. Q. Huang, B. Xiong, X. M. Luo, J. H. Shen, and H. L. Jiang. 2002. Brownian dynamics simulations of the recognition of the scorpion toxin maurotoxin with the voltage-gated potassium ion channels. *Biophys. J.* 83:2370–2385.

13. Orry, A. J., and B. A. Wallace. 2000. Modeling and docking the endothelin G-protein-coupled receptor. *Biophys. J.* 79:3083–3094.

14. Perera, L., C. Foley, T. A. Darden, D. Stafford, T. Mather, C. T. Esmon, and L. G. Pedersen. 2000. Modeling zymogen protein C. *Biophys. J.* 79:2925–2943.

15. Huang, X. Q., J. H. Shen, M. Cui, L. L. Shen, X. M. Luo, K. Ling, G. Pei, H. L. Jiang, and K. X. Chen. 2003. Molecular dynamics simulations on SDF-1α: binding with CXCR4 receptor. *Biophys. J.* 84: 171–184.

16. Filizola, M., M. Carteni-Farina, and J. J. Perez. 1999. Modeling the 3D structure of rhodopsin using a de novo approach to build G-protein-coupled receptors. *J. Phys. Chem. B.* 103:2520–2527.

17. Palczewski, K., T. Kumasaka, T. Hori, C. A. Behnke, H. Motoshima, B. A. Fox, I. Le Trong, D. C. Teller, T. Okada, R. E. Stenkamp, M. Yamamoto, and M. Miyano. 2000. Crystal structure of rhodopsin: a G protein-coupled receptor. *Science.* 289:730–734.

18. Baker, D., and A. Sali. 2001. Protein structure prediction and structural genomics. *Science.* 294:93–96.

19. Teller, D. C., T. Okada, C. A. Behnke, K. Palczewski, and R. E. Stenkamp. 2001. Advances in determination of a high-resolution three-dimensional structure of rhodopsin, a model of G-protein-coupled receptors (GPCRs). *Biochemistry.* 40:7761–7772.

20. Jayasinghe, S., K. Hristova, and S. H. White. 2001. Energetics, stability, and prediction of transmembrane helices. *J. Mol. Biol.* 312: 927–934.

21. Duan, Y., and P. A. Kollman. 1998. Pathways to a protein folding intermediate observed in a 1-microsecond simulation in aqueous solution. *Science.* 282:740–744.

22. Ballesteros, J. A., and H. Weinstein. 1992. Analysis and refinement of criteria for predicting the structure and relative orientations of trans-membranal helical domains. *Biophys. J.* 62:107–109.

23. Accelrys Software Inc. 2000. InsightII, 2000 edition. Accelrys Software, San Diego, CA.

24. Pearson, W. R. 1990. Rapid and sensitive sequence comparison with FASTP and FASTA. *Methods Enzymol.* 183:63–98.

25. Thompson, J. D., D. G. Higgins, and T. J. Gibson. 1994. CLUSTAL W: improving the sensitivity of progressive multiple sequence alignment through sequence weighting, position-specific gap penalties and weight matrix choice. *Nucleic Acids Res.* 22:4673–4680.

26. Berendsen, H. J. C., V. D. Spoel, and R. V. Drunen. 1995. GROMACS: a message-passing parallel molecular dynamics implementation. *Comput Phys Comm.* 95:43–56.

27. Lindahl, E., B. Hess, and V. D. Spoel. 2001. A package for molecular simulation and trajectory analysis. *J. Mol. Mod.* 7:306–317.

28. Aalten, D. M. F., R. Bywater, J. B. Findlay, M. Hendlich, R. W. Hooft, and G. Vriend. 1996. PRODRG, a program for generating molecular topologies and unique molecular descriptors from coordinates of small molecules. *J. Comput. Aided Mol. Des.* 10:255–262.

29. Breneman, C. M., and K. B. Wiberg. 1990. Determining atom-centered monopoles from molecular electrostatic potentials. The need for high sampling density in formamide conformational analysis. *J. Comput. Chem.* 11:361–373.

30. Frisch, M. J. 1998. Gaussian 98, revision A.7. Gaussian, Pittsburgh, PA.

31. Tieleman, D. P., and H. J. C. Berendsen. 1998. A molecular dynamics study of the pores formed by Escherichia coli OmpF porin in a fully hydrated palmitoyloleoylphosphatidylcholine bilayer. *Biophys. J.* 74: 2786–2801.

32. Tieleman, D. P., H. J. C. Berendsen, and M. S. P. Sansom. 1999. An alamethicin channel in a bilayer: molecular dynamics simulations. *Biophys. J.* 76:1757–1769.

33. Faraldo-Gomez, J. D., G. R. Smith, and M. S. P. Sansom. 2002. Setting up and optimization of membrane protein simulations. *Eur. Biophys. J.* 31:217–227.

34. Berendsen, H. J. C., J. P. M. Postma, W. F. Gunsteren, A. DiNola, and J. R. Haak. 1984. Molecular-dynamics with coupling to an external bath. *J. Chem. Phys.* 81:3684–3690.

35. Essmannetal, U., L. Perera, M. L. Berkowitz, T. Darden, H. Lee, and L. G. Pedersen. 1995. A smooth particle mesh Ewald method. *J. Chem. Phys.* 103:8577–8593.

36. Xuan, J. C., G. D. Lin, G. Z. Jin, and Y. Chen. 1988. Relevance of stereo and quantum chemistry of four tetrahydroprotoberberines to their effects on dopamine receptors. *Acta Pharmacol. Sin.* 9:197–205.

37. Morris, G. M., D. S. Goodsell, R. S. Halliday, R. Huey, W. E. Hart, R. K. Belew, and A. J. Olson. 1998. Automated docking using a Lamarckian genetic algorithm and an empirical binding free energy function. *J. Comput. Chem.* 19:1639–1662.

38. Laskowski, R. A., M. W. MacArthur, D. S. Moss, and J. M. Thornton. 1993. PROCHECK: a program to check the stereochemical quality of protein structures. *J. Appl. Crystallogr.* 26:283–291.

39. Vriend, G., and C. Sander. 1993. Quality control of protein models: directional atomic contact analysis. *J. Appl. Crystallogr.* 26:47–60.

40. Cox, B. A., R. A. Henningsen, A. Spanoyannis, R. L. Neve, and K. A. Neve. 1992. Contributions of conserved serine residues in TM5 to the interactions of ligands with dopamine D2 receptors. *J. Neurochem.* 59:627–635.

41. Iwasiow, R. M., M. F. Nantel, and M. Tiberi. 1999. Delineation of the structural basis for the activation properties of the dopamine D1 receptor subtypes. *J. Biol. Chem.* 274:31882–31890.

42. Mo, Y. Q., X. L. Jin, Y. T. Chen, G. Z. Jin, and W. X. Shi. 2005. Effects of I-stepholidine on forebrain Fos expression: comparison with clozapine and haloperidol. *Neuropsychopharmacology.* 30:261–267.

43. Xu, S. X., L. P. Yu, Y. R. Han, Y. Chen, and G. Z. Jin. 1989. Effects of tetrahydroprotoberberines on dopamine receptor subtypes in brain. *Zhongguo Yao Li Xue Bao.* 10:104–110.

44. Dong, Z. J., X. Guo, L. J. Chen, Y. F. Han, and G. Z. Jin. 1997. Dual actions of (−)–stepholidine on the dopamine receptor-mediated adenylate cyclase activity in rat corpus striatum. *Life Sci.* 61:465–472.

45. Peng, C., P. Y. Ayala, H. B. Schlegel, and M. J. Frisch. 1996. Using redundant internal coordinates to optimize geometries and transition states. *J. Comp. Chem.* 17:49–56.

46. Case, D. A., T. E. Cheatham III, T. Darden, H. Gohlke, R. Luo, K. M. Merz, B. Wang, and R. Woods. 2005. The amber biomolecular simulation programs. *J. Computat. Chem.* 26:1668–1688.

47. Amadei, A., A. B. Linssen, and H. J. Berendsen. 1993. Essential dynamics of proteins. *Proteins.* 17:412–425.

48. Roth, B. L., M. Shoham, M. S. Choudhary, and N. Khan. 1997. Identification of conserved aromatic residues essential for agonist binding and second messenger production at 5-hydroxytryptamine2A receptors. *Mol. Pharmacol.* 52:259–266.

49. Woodward, R., S. J. Daniell, P. G. Strange, and L. H. Naylor. 1994. Structural studies on D2 dopamine receptors: mutation of a histidine residue specifically affects the binding of a subgroup of substituted benzamide. *J. Neurochem.* 62:1664–1669.

50. Javitch, J. A., J. A. Ballesteros, H. Weinstein, and J. Chen. 1998. A cluster of aromatic residues in the sixth membrane-spanning segment of the dopamine D2 receptor is accessible in the binding-site crevice. *Biochmestry.* 37:998–1006.

51. Lundstrom, K., M. P. Turpin, C. Large, G. Robertson, P. Thomas, and X. Q. Lewell. 1998. Mapping of dopamine D3 receptor binding site by pharmacological characterization of mutants expressed in CHO cells with the semliki forest virus system. *J. Recept. Signal Transduct. Res.* 18:133–150.

52. Gether, U., and B. K. Kobilka. 1998. G protein-coupled receptors: II. Mechanism of agonist activation. *J. Biol. Chem.* 273:17979–17982.

53. Grobner, G., U. Burnett, C. Glaubitz, G. Cho, A. J. Bason, and A. Watts. 2000. Observations of light-induced structural changes of retinal within rhodopsin. *Nature.* 405:810–813.

54. Shapiro, D. A., K. Kristiansen, W. K. Kroeze, and B. L. Roth. 2000. Differential modes of agonist binding to 5-hydroxytryptamine2A serotonin receptors revealed by mutation and molecular modeling of conserved residues in transmembrane region 5. *Mol. Pharmacol.* 58:877–886.